Karimi, Bayan; He, Hans; Chang, Yu Cheng; Wang, Libin; Pekola, Jukka P.; Yakimova, Rositsa; Shetty, Naveen; Peltonen, Joonas T.; Lara-Avila, Samuel; Kubatkin, Sergey

Electron-phonon coupling of epigraphene at millikelvin temperatures measured by quantum transport thermometry

Published in:
Applied Physics Letters

DOI:
10.1063/5.0031315

Published: 08/03/2021

Document Version
Publisher's PDF, also known as Version of record

Applied Physics Letters

Electron-phonon coupling of epigraphene at millikelvin temperatures measured by quantum transport thermometry

Cite as: Appl. Phys. Lett. **118**, 103102 (2021); https://doi.org/10.1063/5.0031315
Submitted: 29 September 2020 . Accepted: 22 February 2021 . Published Online: 09 March 2021

Bayan Karimi, Hans He, Yu-Cheng Chang, Libin Wang, Jukka P. Pekola, Rositsa Yakimova, Naveen Shetty, Joonas T. Peltonen, Samuel Lara-Avila, and Sergey Kubatkin

Applied Physics Letters ARTICLE scitation.org/journal/apl

Electron-phonon coupling of epigraphene at millikelvin temperatures measured by quantum transport thermometry

Cite as: Appl. Phys. Lett. **118**, 103102 (2021); doi: 10.1063/5.0031315
Submitted: 29 September 2020 · Accepted: 22 February 2021 ·
Published Online: 9 March 2021

View Online Export Citation CrossMark

Bayan Karimi,[1,a)] Hans He,[2] Yu-Cheng Chang,[1] Libin Wang,[1] Jukka P. Pekola,[1,3] Rositsa Yakimova,[4] Naveen Shetty,[2] Joonas T. Peltonen,[1] Samuel Lara-Avila,[2] and Sergey Kubatkin[2]

AFFILIATIONS

[1]Pico group, QTF Centre of Excellence, Department of Applied Physics, Aalto University School of Science, P.O. Box 13500, 00076 Aalto, Finland
[2]Department of Microtechnology and Nanoscience, Chalmers University of Technology, 412 96 Gothenburg, Sweden
[3]Moscow Institute of Physics and Technology, 141700 Dolgoprudny, Russia
[4]Department of Physics, Chemistry and Biology, Linkoping University, 581 83 Linköping, Sweden

[a)]Author to whom correspondence should be addressed: bayan.karimi@aalto.fi

ABSTRACT

We investigate the basic charge and heat transport properties of charge neutral epigraphene at sub-kelvin temperatures, demonstrating a nearly logarithmic dependence of electrical conductivity over more than two decades in temperature. Using graphene's sheet conductance as an *in situ* thermometer, we present a measurement of electron-phonon heat transport at mK temperatures and show that it obeys the T^4 dependence characteristic for a clean two-dimensional conductor. Based on our measurement, we predict the noise-equivalent power of $\sim 10^{-22}\ \mathrm{W}/\sqrt{\mathrm{Hz}}$ of the epigraphene bolometer at the low end of achievable temperatures.

Epitaxial graphene on a SiC substrate (epigraphene) is an attractive scalable[1,2] technology for high-quality graphene electronics.[3–5] Using a recently reported doping technique,[6] epigraphene doped close to the Dirac point has been shown to have great potential for astronomy-oriented terahertz (THz) wave detection, acting as a hot electron bolometric mixer (g-HEB) in heterodyne detection.[4] For g-HEBs, understanding the energy relaxation processes in the material is crucial as it directly impacts the device design and is paramount to achieve high sensitivities and large device bandwidths desired in astronomical observations.[7] In general, decreasing the thermal relaxation rate and heat capacity improves the sensitivity of bolometers and calorimeters;[8,9] this observation has triggered a number of studies on electron-phonon heat transport in graphene at sub-kelvin temperatures.[10–14] For epigraphene, little is known about relaxation processes, particularly when the material is doped close to the Dirac point and in the millikelvin temperature range, conditions at which g-HEBs are expected to perform better. Previous studies of the energy relaxation mechanisms of epigraphene have been mostly limited to samples at high carrier densities and at liquid helium temperatures[15,16] or on micrometer-sized devices where thermalization of hot carriers occurred via the metallic contacts (i.e., diffusion cooling).[4]

Here, we present a study of energy relaxation in charge neutral epigraphene devices fitted with superconducting contacts, which act as thermal barriers that prevent heat leak from the contacts, thus enabling the study of energy relaxation processes in the graphene-silicon carbide system. We use *in situ* thermometry down to sub-100 mK temperatures by measuring the sheet conductance of epigraphene Hall bar devices as they are locally heated by injecting current through Hall probes. This provides a built-in thermometer, and it is made possible by coherent backscattering causing the logarithm in temperature dependence of resistance in lowly doped epigraphene.[4,6,17–20]

Epigraphene was grown on 4H–SiC chips ($7 \times 7\ \mathrm{mm}^2$), which were encased in a graphite crucible and heated by RF heating to around 1850 °C in an inert argon atmosphere of 1 bar.[2] Transmission mode microscopy was used to ensure that the samples had high (>90%) monolayer coverage.[21] Device fabrication utilized standard electron beam lithography techniques, described in detail elsewhere.[22] In short, epigraphene was patterned into Hall bar structures by oxygen plasma etching, and superconducting metallic contacts were prepared with 30 nm-thick aluminum contacts using a 6 nm-thick adhesion layer of titanium. This is a proven technique to make transparent electrical contacts to graphene.[23,24] The metallic layers were deposited by

physical vapor deposition by electron beam evaporation. The finished device was spin-coated with molecular dopants, and the final carrier density was tuned close to charge neutrality by annealing at $T = 160°$ C.[6] In order to test the device quality, initial DC electrical characterization was performed using quantum Hall measurements on a PPMS (Physical Property Measurement System from Quantum design) liquid helium cryostat (2–300 K) with a superconducting magnet providing fields up to 14 T. Sub-kelvin measurements were performed in a dilution refrigerator.

Figure 1(a) shows an optical micrograph of the doped epigraphene Hall bar used for our study, with channel length $L = 250\,\mu$m and width $w = 50\,\mu$m. Quantum Hall measurements at 2 K were used to verify the quality of the devices [Fig. 1(b)]. The sample shows fully developed quantum Hall effects, with vanishing longitudinal resistance $R_{XX} = 0$ and quantized transverse resistance $R_{XY} = h/2e^2$. This proves that the sample is of high quality monolayer epigraphene with spatially homogenous doping.[6,25,26] The device is p-doped, with a carrier density of $p = 1.7 \times 10^{10}$ cm^{-2} and a mobility of $\mu = 14500$ cm^2/V s.

In Fig. 2(a), we show the current–voltage (IV) characteristics measured in a dilution refrigerator at various temperatures ranging from about 50 mK up to 550 mK. The four-probe configuration for these measurements is shown in the inset of Fig. 2(a). The temperature dependence of zero-bias differential sheet conductance of the device is seen in Fig. 2(b), extracted from the average slope of the IV curve over a current range of a few pA around zero current. The vertical scale on the right (shown in pink color) is the sheet conductance expressed in units of the conductance quantum $\sigma_0 = e^2/h$. The inset of Fig. 2(b) shows the temperature dependence of the sheet conductance in a wider temperature range. Data in the two separate ranges of temperature were measured using different setups. We observe approximately a logarithmic-in-temperature dependence of the sheet conductance of graphene, $\sigma(T) = \sigma_1 + A\sigma_0 \ln(T)$, with $\sigma_0 = e^2/h \approx 3.9 \times 10^{-5}$ S, where e is the elementary charge and h is the Planck constant. The slope of the logarithmic term quantifies the strength of the quantum corrections in the material, and for this p-doped sample, $A \approx 0.69$, higher than $A \approx 0.30$ reported for n-doped samples.[4] Studies in a magnetic field would be required to verify if a higher A is the result of enhanced electron-electron interactions or quantum interference effects in p-doped samples.[27]

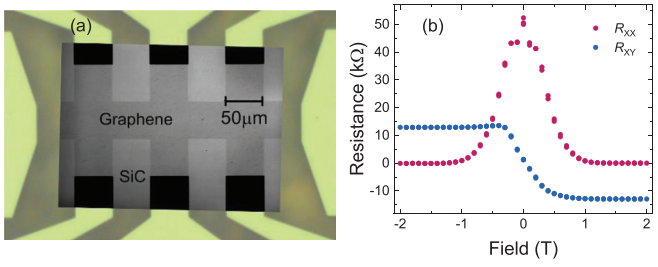

FIG. 1. Hall bar device with doped epigraphene. (a) Optical micrograph showing the Hall bar device ($L = 250\,\mu$m and $w = 50\,\mu$m). The center overlay shows an image taken in transmission mode, which enables visualizing epigraphene. (b) Example of DC electrical characterization of the epigraphene Hall bar with hole type carrier density $p = 1.7 \times 10^{10}$ cm^2, measured using $I = 100$ nA and $T_0 = 2$ K. The sample demonstrates the fully developed quantum Hall effect with $R_{XX} = 0$ and $R_{XY} = h/2e^2$, the hallmark of monolayer graphene in magnetotransport.

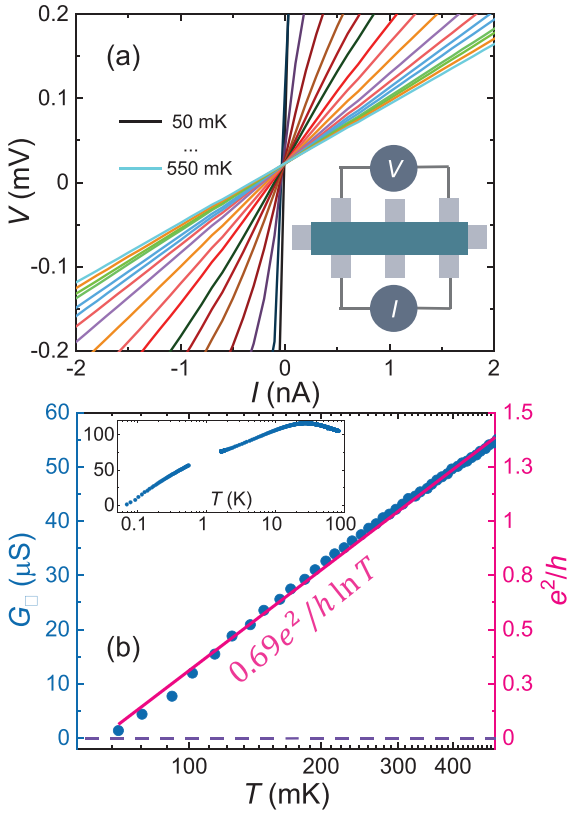

FIG. 2. Low temperature electrical transport measurement of epigraphene. (a) Current–voltage characteristics (IV) measured in a four-probe configuration (inset) across the entire graphene channel. The different curves correspond to different temperatures from dark to light such that the steepest one is for $T = 50$ mK and the one with the smallest slope for $T = 550$ mK with the intermediate curves taken at temperatures in between. (b) Zero bias differential sheet conductance on the logarithmic temperature scale in the same range as in (a). The inset displays the same measurements in a wider range of temperatures. The pink line shows the logarithmic fit to the experimental data.

For thermal characterization of the device [see the upper inset of Fig. 3(a)], we have considered four contributions when analyzing the local thermal balance of the epigraphene structure. They are (i) the thermal conductance from epigraphene to the phonon bath G_{th}, (ii) the lateral thermal conductance along the epigraphene sheet κ, (iii) the thermal conductance of the substrate partly shunting thermally the epigraphene (G_{SiC}), and finally (iv) the thermal conductance to the superconducting leads (G_{out}) to which the Hall bar structure is connected. For an ideal measurement of epigraphene properties only, the two first ones ought to dominate, and the two others should not contribute to the heat currents. Yet, as we argue below, our measurements, together with estimates of substrate material properties, and assuming that the Wiedemann-Franz law is approximately valid for epigraphene, the shunting effect (iii) exceeds the thermal conductance along the epigraphene sheet by several orders of magnitude.

In the measurements of the hot electron effect in the epigraphene device, depicted in the lower inset of Fig. 3(a), the Joule power $P = IV$ generated by the bias current leads to an increase in the electronic temperature of graphene, which is measured through monitoring the sheet

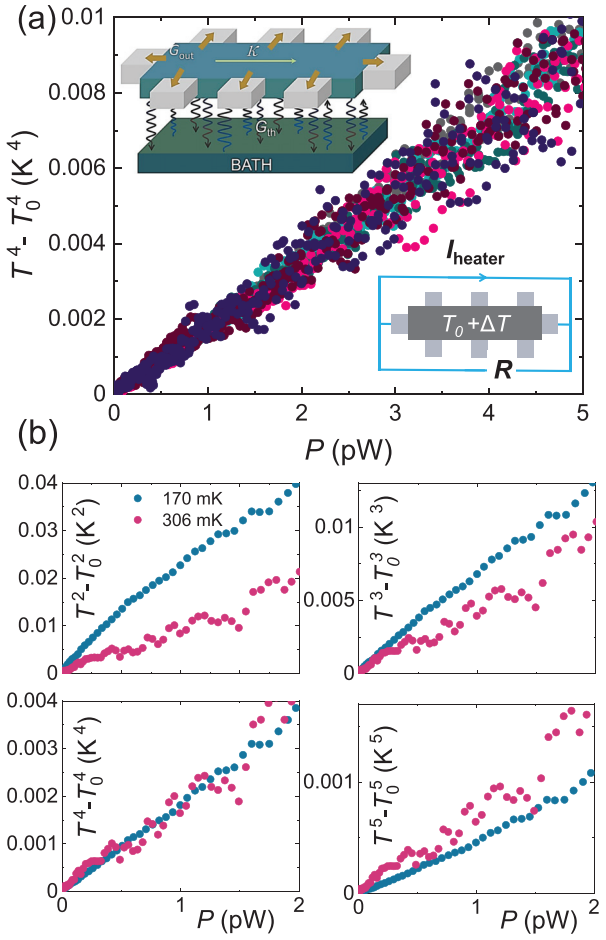

FIG. 3. Electron phonon coupling in epigraphene doped close to the Dirac point. (a) The upper inset shows the various heat transport components: the dominant one is the conductance to the phonon bath, G_{th}, and we can neglect the lateral conductance κ and the leak into the leads G_{out}. The mainframe shows the power $P = IV$ dependence of the difference in the fourth power of the temperatures of the epigraphene electrons and the substrate, T_e and T_0, respectively. The substrate temperatures range from 170 to 306 mK for each dataset shown in different colors. The setup for this measurement is schematically presented in the lower inset. (b) Demonstration that the heat flow indeed obeys the law $P = \Sigma_4 A(T_e^4 - T_0^4)$ for graphene in the clean limit. The difference $T_e^n - T_0^n$ has been plotted for $n = 2$, 3, 4, and 5 at $T_0 = 170$ mK (blue symbols) and $T_0 = 306$ mK (pink symbols).

conductance of the material. With superconducting aluminum contacts, the heat flow through the contacts is $G_{out} \propto e^{-\Delta/k_B T}$,[28–30] where $\Delta \simeq 200\ \mu$eV. Then, at $T \lesssim 0.3$ K of our measurement, this heat flow is negligibly small, and the only energy relaxation pathway in the system is to the phonon bath [i.e., item (i)]. The main panel of Fig. 3(a) is a collection of such measurements in the temperature range from 170 mK to 306 mK, showing that the heat flux P from the electron system at temperature T_e to the phonon bath (at constant bath temperature T_0) follows the law

$$P_{ep} = \Sigma_n A(T_e^n - T_0^n), \tag{1}$$

with $n = 4$ and $\Sigma_4 \approx 0.04\ \mathrm{WK^{-4}\ m^{-2}}$. This power law is consistent with theoretical predictions for graphene in the clean limit[11,13] and with previous reports in highly n-doped epigraphene ($n = 1.63 \times 10^{12}$ cm^{-2}) and at temperatures up to $T = 10$ K.[15,16] The four sets of plots presented in Fig. 3(b) demonstrate a similar dependence but with only the extreme bath temperatures (170 and 306 mK) and with different power laws $n = 2$, 3, 4, and 5. Only data with T^4 collapse on the same slope at the two bath temperatures. It is evident that $n = 4$ describes our experiment best.

The electrical conductance across the Hall bar, e.g., between two adjacent Hall probes with a distance of $\sim 50\ \mu$m, is $G \sim 10^{-5}\ \Omega^{-1}$ [see Fig. 2(b)]. Using the Wiedemann-Franz law, we obtain $\kappa = G\mathcal{L}_0 T \simeq 4 \times 10^{-14}$ W/K for the thermal conductance in this geometry at $T = 0.2$ K. Here, $L_0 = 2.4 \times 10^{-8}\ \mathrm{W\,\Omega\,K^{-2}}$ is the Lorenz number. It is, then, evident that the electron-phonon conductance dominates and shunts the system thermally under the same conditions $G_{th} \equiv dP_{ep}/dT_e = 4\Sigma_4 A_{\square} T_e^3 \sim 3 \times 10^{-12}$ W/K for the area under the heater. Since the thermal conductance of the 3D structure is large, we conclude that the role of κ is negligible in our measurements. However, the low value of κ means that for quantitative analysis of the data, we need to take into account that only the seven squares in the current path of the 19 squares in the whole structure are heated.

The thermal characterization allows us to calculate the noise-equivalent power (NEP), an important figure of merit of a bolometer. In the limit where this figure is determined by fundamental energy fluctuations, it assumes value NEP $= 2\sqrt{G_{th} k_B T^2}$. In our case $G_{th} = 4\Sigma_4 A T^3$ from the electron-phonon measurement, $T = 170$ mK, and $A = 4 \times 45 \times 45 \times 10^{-12}$ m^2, we obtain NEP $\sim 3 \times 10^{-18}\ \mathrm{W}/\sqrt{\mathrm{Hz}}$. This is still not record-low because of the large area in our sample and relatively high T. In order to improve the NEP, one needs to reduce the area of the detector and operate it at lower T. One can realistically make $A \sim 10^{-11}$ m^2 and operate at about 10 mK. In this case, the projected NEP $\sim 10^{-22}\ \mathrm{W}/\sqrt{\mathrm{Hz}}$, which would outperform the current experimental state-of-the-art.[8] Although here we do not present heat transport data below 170 mK, we believe that lower T measurements are feasible: applying a moderate magnetic field of ~ 50 mT perpendicular to the graphene sheet restores the conductance of it down to $T = 10$ mK. The detector can be impedance-matched to the photon source by proper choice of the aspect ratio of the resistive element as was done in Ref. 4, allowing for RF readout up to 8 GHz. Other RF-readout schemes providing other bandwidths such as that in Ref. 31 might be implemented.

In summary, we have demonstrated sensitive *in situ* thermometry by measuring the sheet conductance of the epigraphene sheet down to sub-100 mK temperatures, providing a way for sensitive calorimetry with a built-in thermometer. The $P \propto T^4$ dependence observed in our measurements for charge-neutral graphene at mK temperatures in fact coincides with previous observations in epigraphene at high doping and temperatures well above 1 K[15,16] and in charge-neutral graphene down to 300 mK.[4] For epigraphene, it has been established that a low-energy remote interfacial mode is responsible for scattering, and this mode originates from the interaction between graphene and the buffer layers oscillating out-of-phases parallel to each other.[32–34] Our experiments indicate that the T^4 trend extends down to $T = 50$ mK. The coupling of the epigraphene electrons to the phonon bath dies off more slowly with decreasing temperature than in metal films ($T^3 \ldots T^4$ vs $T^4 \ldots T^6$);[35] therefore, the advantage in operating at the very low temperatures is not quite that obvious in the case of epigraphene as compared to metals, where

furthermore the proximity superconductivity can be used for enhancement of sensitivity. Yet, the extremely small heat capacity of the epigraphene sheets at low temperatures leads to very fast thermal relaxation times of the order of 10 ps, making, together with *in situ* thermometry and weak G_{th}, the epigraphene bolometer an attractive choice for terahertz applications.

This work was jointly supported by the Swedish Foundation for Strategic Research (SSF) (Nos. GMT14-0077 and RMA15-0024), Chalmers Excellence Initiative Nano, and European Union's Horizon 2020 research and innovation program under Marie Sklodowska-Curie Grant Agreement No 766025. This work was performed in part at Myfab Chalmers. We acknowledge the facilities and technical support of Otaniemi Research Infrastructure for Micro and Nanotechnologies (OtaNano). We thank the Russian Science Foundation (Grant No. 20-62-46026) for supporting this work. This research made use of the OtaNano–Low Temperature Laboratory infrastructure of Aalto University, which is part of the European Microkelvin Platform EMP (funded by European Union's Horizon 2020 Research and Innovation Programme, Grant No. 824109).

DATA AVAILABILITY

The data that support the findings of this study are available from the corresponding author upon reasonable request.

REFERENCES

[1]K. V. Emtsev, A. Bostwick, K. Horn, J. Jobst, G. L. Kellogg, L. Ley, J. L. McChesney, T. Ohta, S. A. Reshanov, J. Röhrl, E. Rotenberg, A. K. Schmid, D. Waldmann, H. B. Weber, and T. Seyller, Nat. Mater. **8**, 203 (2009).
[2]C. Virojanadara, M. Syväjarvi, R. Yakimova, L. Johansson, A. Zakharov, and T. Balasubramanian, Phys. Rev. B **78**, 245403 (2008).
[3]A. Tzalenchuk, S. Lara-Avila, A. Kalaboukhov, S. Paolillo, M. Syväjärvi, R. Yakimova, O. Kazakova, T. J. B. M. Janssen, V. Fal'ko, and S. Kubatkin, Nat. Nanotechnol. **5**, 186 (2010).
[4]S. Lara-Avila, A. Danilov, D. Golubev, H. He, K. H. Kim, R. Yakimova, F. Lombardi, T. Bauch, S. Cherednichenko, and S. Kubatkin, Nat. Astron. **3**, 983 (2019).
[5]H. He, S. Lara-Avila, K. H. Kim, N. Fletcher, S. Rozhko, T. Bergsten, G. Eklund, K. Cedergren, R. Yakimova, Y. W. Park, A. Tzalenchuk, and S. Kubatkin, Metrologia **56**, 045004 (2019).
[6]H. He, K. H. Kim, A. Danilov, D. Montemurro, L. Yu, Y. W. Park, F. Lombardi, T. Bauch, K. Moth-Poulsen, T. Iakimov, R. Yakimova, P. Malmberg, C. Müller, S. Kubatkin, and S. Lara-Avila, Nat. Commun. **9**, 3956 (2018).
[7]T. M. Klapwijk and A. V. Semenov, IEEE Trans. Terahertz Sci. Technol. **7**, 627–648 (2017).
[8]R. Kokkoniemi, J. Govenius, V. Vesterinen, R. E. Lake, A. M. Gunyhó, K. Y. Tan, S. Simbierowicz, L. Grönberg, J. Lehtinen, M. Prunnila *et al.*, "Nanobolometer with ultralow noise equivalent power," Commun. Phys. **2**, 124 (2019).
[9]B. Karimi, F. Brange, P. Samuelsson, and J. P. Pekola, "Reaching the ultimate energy resolution of a quantum detector," Nat. Commun. **11**, 367 (2020).
[10]D. K. Efetov, R.-J. Shiue, Y. Gao, B. Skinner, E. D. Walsh, H. Choi, J. Zheng, C. Tan, G. Grosso, C. Peng, J. Hone, K. C. Fong, and D. Englund, Nat. Nanotechnol. **13**, 797 (2018).
[11]F. Vischi, M. Carrega, A. Braggio, F. Paolucci, F. Bianco, S. Roddaro, and F. Giazotto, Phys. Rev. Appl. **13**, 054006 (2020).
[12]I. V. Borzenets, U. C. Coskun, H. T. Mebrahtu, Y. V. Bomze, A. I. Smirnov, and G. Finkelstein, Phys. Rev. Lett. **111**, 027001 (2013).
[13]X. Du, D. E. Prober, V. Heli, and C. B. Mckitterick, Graphene 2D Mater. **1**, 1 (2014).
[14]K. C. Fong, E. E. Wollman, H. Ravi, W. Chen, A. A. Clerk, M. D. Shaw, H. G. Leduc, and K. C. Schwab, Phys. Rev. X **3**, 041008 (2013).
[15]A. M. R. Baker, J. A. Alexander-Webber, T. Altebaeumer, S. D. McMullan, T. J. B. M. Janssen, A. Tzalenchuk, S. Lara-Avila, S. Kubatkin, R. Yakimova, C.-T. Lin, L.-J. Li, and R. J. Nicholas, Phys. Rev. B **87**, 045414 (2013).
[16]J. Huang, J. A. Alexander-Webber, T. J. B. M. Janssen, A. Tzalenchuk, T. Yager, S. Lara-Avila, S. Kubatkin, R. L. Myers-Ward, V. D. Wheeler, D. K. Gaskill, and R. J. Nicholas, J. Phys.: Condens. Matter **27**, 164202 (2015).
[17]S. V. Morozov, K. S. Novoselov, M. I. Katsnelson, F. Schedin, L. A. Ponomarenko, D. Jiang, and A. K. Geim, "Strong suppression of weak localization in graphene," Phys. Rev. Lett. **97**, 016801 (2006).
[18]E. McCann, K. Kechedzhi, V. I. Fal'ko, H. Suzuura, T. Ando, and B. L. Altshuler, "Weak-localization magnetoresistance and valley symmetry in graphene," Phys. Rev. Lett. **97**, 146805 (2006).
[19]F. V. Tikhonenko, A. A. Kozikov, A. K. Savchenko, and R. V. Gorbachev, "Transition between electron localization and antilocalization in graphene," Phys. Rev. Lett. **103**, 226801 (2009).
[20]K. Kechedzhi, D. W. Horsell, F. V. Tikhonenko, A. K. Savchenko, R. V. Gorbachev, I. V. Lerner, and V. I. Fal'ko, "Quantum transport thermometry for electrons in graphene," Phys. Rev. Lett. **102**, 066801 (2009).
[21]T. Yager, A. Lartsev, S. Mahashabde, S. Charpentier, D. Davidovikj, A. Danilov, R. Yakimova, V. Panchal, O. Kazakova, A. Tzalenchuk, S. Lara-Avila, and S. Kubatkin, Nano Lett. **13**, 4217 (2013).
[22]A. Tzalenchuk, S. Lara-Avila, K. Cedergren, M. Syväjärvi, R. Yakimova, O. Kazakova, T. Janssen, K. Moth-Poulsen, T. Bjørnholm, S. Kopylov, V. Fal'ko, and S. Kubatkin, Solid State Commun. **151**, 1094 (2011).
[23]H. B. Heersche, P. Jarillo-Herrero, J. B. Oostinga, L. M. K. Vandersypen, and A. F. Morpurgo, Nature **446**, 56 (2007).
[24]N. Mizuno, B. Nielsen, and X. Du, Nat. Commun. **4**, 2716 (2013).
[25]S. Cho and M. S. Fuhrer, Phys. Rev. B **77**, 081402(R) (2008).
[26]R. P. Tiwari and D. Stroud, Phys. Rev. B **79**, 165408 (2009).
[27]S. Lara-Avila, A. Tzalenchuk, S. Kubatkin, R. Yakimova, T. J. B. M. Janssen, K. Cedergren, T. Bergsten, and V. Fal'ko, Phys. Rev. Lett. **107**, 166602 (2011).
[28]J. Bardeen, G. Rickayzen, and L. Tewordt, "Theory of the thermal conductivity of superconductors," Phys. Rev. **113**, 982 (1959).
[29]J. T. Peltonen, P. Virtanen, M. Meschke, J. V. Koski, T. T. Heikkilä, and J. P. Pekola, "Thermal conductance by the inverse proximity effect in a superconductor," Phys. Rev. Lett. **105**, 097004 (2010).
[30]A. V. Timofeev, M. Helle, M. Meschke, M. Möttönen, and J. P. Pekola, "Electronic refrigeration at the quantum limit," Phys. Rev. Lett. **102**, 200801 (2009).
[31]R. J. Schoelkopf, P. Wahlgren, A. A. Kozhevnikov, P. Delsing, and D. E. Prober, Science **280**, 1238 (1998).
[32]S. Tanabe, Y. Sekine, H. Kageshima, M. Nagase, and H. Hibino, "Carrier transport mechanism in graphene on SiC(0001)," Phys. Rev. B **84**, 115458 (2011).
[33]N. Ray, S. Shallcross, S. Hensel, and O. Pankratov, "Buffer layer limited conductivity in epitaxial graphene on the Si face of SiC," Phys. Rev. B **86**, 125426 (2012).
[34]J. Huang, J. A. Alexander-Webber, A. M. R. Baker, T. J. B. M. Janssen, A. Tzalenchuk, V. Antonov, T. Yager, S. Lara-Avila, S. Kubatkin, R. Yakimova, and R. J. Nicholas, "Physics of a disordered Dirac point in epitaxial graphene from temperature-dependent magnetotransport measurements," Phys. Rev. B **92**, 075407 (2015).
[35]F. Giazotto, T. T. Heikkilä, A. Luukanen, A. M. Savin, and J. P. Pekola, Rev. Mod. Phys. **78**, 217 (2006).